International Journal of Artificial Intelligence and Emerging Technology (2024) ,(2) 42–52
ISSN 2735-4792 (Print); 2735-4806 (Online)
International Journal of Artificial Intelligence and Emerging Technology
Available online at : https://ijaeur.journals.ekb.eg/

Ahmed G. Mahmoud A. Aziz

Electrical and Computers Engineering Department, Higher Institute of Engineering and Technology, New Minya, Egypt.

Corresponding author: E-mail: a.g.mahmoud@mhiet.edu.eg

Keywords:
AIS, GIS, AI, Partial Discharge, Support Vector Machine, Random Forest

A Robust Machine Learning Framework for Partial Discharge Diagnosis in Diverse Power Substations

ABSTRACT
Partial discharge (PD) detection is essential to avoid failures in electrical substations. This paper focuses on classifying PD types in both Air-Insulated (AIS) and Gas-Insulated (GIS) substations. Support Vector-Machine (SVM) and Random Forest (RF), two artificial intelligence (AI) methods, were created for this task. The paper provides the complete mathematical framework for two distinct machine learning (ML) classifiers specifically designed for subtraction analysis. The three primary PD-sources: corona, surface, and internal discharge were recognized by the models during training. The study validates the PD-features by analyzing and presenting distinct time-domain waveforms and frequency-domain spectra for each discharge type under noisy-conditions, providing a strong physical basis for the AI-classification. The RF-classifier achieved perfect accuracy of 99.6%. The SVM-classifier also showed high accuracy of 97.78%. The results demonstrate that AI can provide reliable early warning for substation maintenance. This helps improve the safety and reliability of power networks. The research offers a practical framework for applying these methods in Egypt's energy sector.

1. Introduction

The demand for advanced substation monitoring, diagnostic, and control technology has increased due to the complexity of contemporary power systems. The foundations of transmission and distribution networks, where performance, effectiveness, and safety are critical, are represented by gas-insulated substations (GIS) and air-insulated substations (AIS). Traditional monitoring-systems have frequently depended on manual interventions and threshold-based-alerts, which have limitations in terms of their capacity to anticipate breakdowns or improve performance in real time. To isolate and protect and high-voltage-substations, these designs use insulating gases, most frequently sulfur hexafluoride (SF_6), inside tight enclosures. The AIS, on the other hand, use ambient air as the main insulating-medium and frequently need for a larger layout [1].

The three primary origins of partial discharge (PD) are surface discharges (SD), corona discharges (CD), and internal-discharges (ID), according to [2]. The CDs appear in areas where there is a strong electric-field among the conductor and the surrounding air or in pointed conductive-materials. Since they are exterior, these discharges typically do not indicate the insulation-deterioration. Conversely, the SDs happen at the interface among an insulating-material with air and are frequently brought on by unfavorable environmental-factors; mechanical wear, or pre-existing deterioration of the insulating-material. Finally, internal-discharges occur in cavities that are incorporated into the insulating-substance. These cavities make it easier for areas with strong electric-fields to grow, which can gradually deteriorate the material until serious failures happen. For efficient fault-identification and insulation system evaluation, it is essential to comprehend these various PD-sources [3].

High-voltage substations are being modified more and more by artificial intelligence (AI), which improves predictive-maintenance, intelligent-fault-detection, and operational-reliability. Large amounts of monitoring data produced by substation sensors and supervisory systems can be analyzed with the use of contemporary AI techniques like

machine learning (ML) and deep learning (DL) [4, 5]. Since convolutional neural-networks (CNNs) attained state-of-the-art performance in image-classification tasks in 2012, DL, which has its roots in artificial neural-network (ANN) research , has seen incredible advancements [4]. These developments have opened the door for the use of DL models in fields well outside computer-vision, such as substation-automation and power-system-diagnostics.

2. Literature Review

A breakdown condition known as PD is linked to electrical-insulation that has weak areas or defects. Electrical discharges occur in defective-places; partially spanning the space among conductors, even while the majority of the insulation, for instance, in a generator can sustain the electric forces experienced [6]. This only occurs when the electric field strength is greater than the insulating material's breakdown strength, which is typically the result of localized deterioration. High-frequency, transient currents that last only a few nanoseconds to microseconds are produced when the arc leaps through the void. Light, heat, sound, high-frequency waves, and chemical processes that might result in the production of ozone and other gases are all produced by PD [7]. The PD will deteriorate insulation over time. The insulation will develop conductive-channels, which will cause PD to worsen. The obvious effect of the injury is treeing, or the development of conductive-pathways that resemble trees with numerous branches [6].

PD is frequently regarded as a key symptom of electrical-equipment non-conformities and is invariably linked to insulation problems [8]. To identify issues and evaluate the operational state of electrical system assets, PD-analysis is suggested in a number of studies [2, 3, 5, 7, 9, 10]. Although PD measures present a viable method for assessing insulation-system-deterioration, the literature generally recognizes a number of restrictions on their use, particularly when conducting measurements online [4, 9, 11]. Corona, Radio waves, TV transmissions, WiFi, and other ambient elements can interfere with sensors that are used to measure PD. A major obstacle in this area of study is the existence of several PD sources, which further complicates fault-detection. Distinguishing among various PD types and separating them from other noise sources becomes a crucial difficulty in this field of study. The ensuing pulse's waveform properties can be affected by the discharge's source as well as the insulating-material in which it occurs. As a result, many studies have put forth methods for identifying and differentiating discharge sources through the analysis of pulse-extracted features [9, 11].

Utilizing traits associated with the PRPD-pattern (Phase-Resolved PD) is one way employed for this aim. The PRPD-pattern is helpful for categorizing discharge types since it typically stays the same for every kind of discharge [2, 12, 13]. However, PRPD-patterns become more complicated and challenging to understand when there are several discharge sources or significant noise, which is common in substation measurements. Another strategy is to classify pulse sources according to similar-characteristics. Features pertaining to pulse-form, frequency, and duration are typically employed. PRPD-patterns can be separated by classifying pulses according to their similarity [14, 15]. The development of tools for automatic-monitoring of the existence of PD can be facilitated by the combination of supervised models for categorizing PRPD-patterns and unsupervised models for differentiating discharge sources [16, 17].

New potential and challenges for GIS fault-diagnosis are presented by the development of the powerless Internet-of-Things (IoT) [18, 19]. The capacity to accurately identify fault-diagnosis techniques for GIS faults, as well as the exploration of real-time rapid processing of GIS fault signals, has emerged as a pressing issue that requires immediate attention. Statistics show that insulation flaws are the primary cause of GIS accidents [20], and the majority of these flaws show up as PD, which will hasten the aging of equipment. Presently, the primary methods for identifying insulation flaws are the measurement of light-scale, sound, heat, and electromagnetic-waves as well as the breakdown of chemical compounds brought on by PD [21]. Pulse current, ultrasonic, ultra

high-frequency (UHF), optical-detection, and gas-decomposition product detection are some of the detection techniques [22-24]. The UHF approach is the most popular of these techniques due to its great detection sensitivity and potent anti-interference capability [25]. Conventional ML techniques do exceptionally well in the classification of PD-patterns. However, their feature extraction techniques over-rely on expert knowledge, and extensive human labor will result in unintentional mistakes. It is challenging to ensure that features retrieved by various algorithms remain the best in other methods because they are neither transportable nor shared [26]. The DL techniques that rely on automatic feature extraction are incorporated with GIS PD-pattern recognition to effectively address this issue. Currently, one-dimensional convolution, LeNet5, AlexNet, and long short-term memory (LSTM) models are among these DL models [12, 27, 28].

Overheating and abnormal discharges in GIS produce breakdown products, such as SO_2, SOF_2, SO_2F_2, and H_2S. Adsorption mechanisms and sensor selectivity are examined in first-principles and experimental investigations. The data can be used with PD sensing to estimate fault severity and infer fault type [7, 29].

The following are the primary contributions of this paper:

- Providing a foundational characterization of the three primary PD-types (Corona, Surface, Internal) relevant to AIS and GIS environments, which is essential for accurate AI classification.
- Application of AI Models: This study successfully applied two ML models, Support Vector Machine (SVM) and Random Forest (RF), to PD-types in substations.
- Customized Model Implementation: The study showed how each model was specifically appropriate for various substation conditions. While RF demonstrated high efficiency with clear signal data, SVM performed well in noisy-environments.
- High Classification Accuracy: The implemented models achieved outstanding performance. The SVM-classifier reached an accuracy of 97.78%, and the RF-classifier achieved a perfect accuracy of 99% in classifying corona, surface, and internal discharges.
- Comprehensive Performance Validation: The study provided a full evaluation using standard-metrics (Precision, Recall, F1-Score), confirming the reliability and robustness of both AI classifiers for PD analysis.

3. Electrical Energy Generation

A. Energy in Generation Egypt

Due to large capacity additions, Egypt has established a notable surplus in power generation. With an increasing tendency toward GIS in strategic and urban projects, the decision between AIS and GIS is based on a crucial trade-off between initial cost, spatial-needs, and operational-reliability.

In 2022/2023, Egypt's installed generating capacity totaled 59,442 MW [30]. Thermal sources, such as natural gas and petroleum products, accounted for 87.93% (190.15 TWh) of the total energy output, which came to 216.25 TWh. Hydropower (15.4 TWh), wind (1,632.3 MW capacity), and solar (1,674 MW capacity, including the 1,465 MW Benban Solar Park) were the renewable-energy-sources that accounted for 12.1% of the total [30, 31].

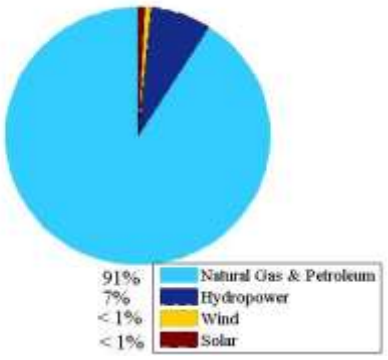

Figure 1: Electricity generation in Egypt (2022/2023)

As of June 2023, this represents a 14.2% annual increase in energy-generation and

consumption [32, 33]. With an output of 220.1 TWh in 2023, Egypt was the second-largest generator of electricity in the Arab world [31, 32].

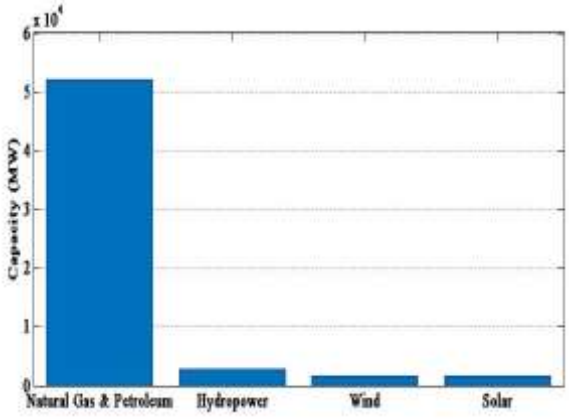

Figure 2: Installed Electricity Capacity in Egypt (2022/2023)

B. Substation Technology in Egypt

As of June 2023, the transmission-network has a volume of 199,517 MVA and a circuit length of 57500 km [30]. Although there is no publicly available official count of AIS and GIS units, industry trends and project data show a distinct technology segmentation: AIS are still widely used because of their lower initial capital expense. They are usually used in projects with a tight-budget, for distribution-level voltages, and in rural and semi-urban locations with lots of space [34, 35]. GIS is being used more and more in strategic, contemporary initiatives. Their main benefit is a drastically smaller footprint (up to 70% smaller than AIS), which makes them perfect for places with tough-environmental-conditions (like dusty, coastal areas) and dense metropolitan areas (like Cairo, Alexandria) [28, 35]. Because of their sealed construction, which shields components from weather and pollutants, they are more reliable and require less maintenance; nonetheless, they use SF_6 gas, which has a significant potential to cause global warming [7, 36]. A clear comparison of the two technologies is given in **Table** 1 [36-39]:

Table **2**: Air and Gas-insulated Substations

Criterion	AIS	GIS
Insulation Medium	Air	SF_6
Space Requirement	Large	Compressed
Maintenance	Frequent	Low
Cost	Lower	Higher
Reliability	Moderate	High
Environmental Impact	Minimal	High due to SF_6

Egypt's electricity-industry has shown strong growth and a deliberate extension of its grid-infrastructure. GIS and AIS technologies are anticipated to continue to coexist. In traditional applications, AIS is preferred due to its cost-effectiveness, while GIS is becoming more and more popular in metropolitan-areas, vital infrastructure, and connectivity projects due to its dependability and spatial-efficiency. Future developments will probably see a slow transition to SF_6-free GIS-technology as they become more economically feasible and in line with international environmental-sustainability objectives [35, 36].

4. Types of Partial Discharges Taken into Account by AIS and GIS

There are three main types of PD that are pertinent to HV substations: corona, surface, and internal discharges. The manifestation of PD varies based on the insulation-medium and the location of the defect. For accurate insulation diagnostics in both AIS and GIS, these categories are essential.

4.1 Corona Discharge

Corona is a localized discharge occurring around sharp-edges or protrusions where the electric-field-intensity exceeds the inception threshold of the surrounding medium (typically air or SF_6). It is characterized by low-energy, fast-rise pulses with short-decay constants. The discharge magnitude is relatively small, but its continuous occurrence accelerates aging and leads to electromagnetic-interference [2].

$$i_c(t) = A_c\,(e^{-t/\tau_c})\,\sin(2\pi f_c t), \quad t \geq 0 \qquad (1)$$

4.2 Surface Discharge

Surface PD happens along dielectric-boundaries, particularly when there is moisture or pollution present. As the charge disperses along the dielectric-contact, the discharges have a larger duration and an

intermediate magnitude in comparison to corona [2, 11].

$$i_s(t) = A_s\,(e^{-t/\tau_s})\,\sin(2\pi f_s t), \quad t \geq 0 \qquad (2)$$

4.3 Internal Discharge

Internal PD develops in solid insulation's gas-filled holes or cavities. These discharges are a crucial symptom of insulation deterioration since they are high-energy-occurrences with a considerable charge size and a comparatively long-duration [2].

$$i_i(t) = A_i\,(e^{-t/\tau_i})\,\sin(2\pi f_i t), \quad t \geq 0 \qquad (3)$$

To approximate the fast-rise-time and slower decay typically observed in PD-events [13], a double-exponential-formulation is used:

$$v(t) = A\left(e^{-\alpha t} - e^{-\beta t}\right)\sin(2\pi f t), \quad t \geq 0 \qquad (4)$$

where, A is the discharge-amplitude, proportional to discharge-magnitude (pC), α represents the slow-decay-constant and β represents the fast-rise-constant ($\beta \gg \alpha$)

TABLE **2**: COMPARATIVE CHARACTERISTICS OF MAJOR PD TYPES IN AIS AND GIS

PD Type	Pulse Amplitude	Decay Constant (τ)	Dominant Frequency
Corona	Low (<1 pC to few pC)	Sub-µs (0.5–1 µs)	High (tens of MHz)
Surface	Medium (few pC to tens of pC)	Few µs (1–3 µs)	Medium (MHz range)
Internal	High (tens to hundreds of pC)	Several µs (3–10 µs)	Lower (hundreds of kHz–few MHz)

The pulse charge and decay constant values in TABLE 2 are derived from studies on PD in AIS and GIS insulation-systems as well as typical ranges published in IEEE Std 400.3 and IEC 60270 [37, 39]. Although they are representative parameters for simulation and classification, the listed ranges are not absolute.

The theoretical basis for feature extraction and AI-based classification of PD signals in this study utilizing ML and DL models (SVM, RF, CNN, LSTM) is provided by the distinctive characteristics of amplitude, decay constant (τ), and frequency spectrum.

5. AI Classifier Mathematical Modeling for PD Analysis in AIS and GIS

AI methods have become effective tools for PD-classification and detection in both AIS and GIS. In addition to offering a foundation for classification-accuracy, the mathematical-formulation of ML/DL models offers theoretical insights into how well they operate in various operational scenarios and noise levels. SVM and Random Forests (RF) are the representative AI classifiers whose mathematical underpinnings are presented in this section along with their applicability to PD analysis in AIS and GIS.

5.1 Support Vector Machine (SVM)

Since SVMs can create the best separating hyperplanes in high-dimensional-feature spaces, they are frequently employed in electrical engineering for classification problems. They are especially well-suited for differentiating PD sources in AIS and GIS systems due to their resilience to noise [40].

For training data $(\mathcal{X}_i, \mathcal{Y}_i)$, where $\mathcal{X}_i \in \mathbb{R}^n$ and $\mathcal{Y}_i \in \{-1, +1\}$:

$$\min_{w,b,\xi} \frac{1}{2}\|w\|^2 + C\sum_{i=1}^{N}\xi_i \qquad (5)$$

Subject to:

$$\mathcal{Y}_i\,(w.\mathcal{X}_i + b) \geq 1 - \xi_i\,, \quad \xi_i \geq 1 \qquad (6)$$

The decision function is:

$$f(x) = sign\left(\sum_{i=1}^{N}\alpha_i\,\mathcal{Y}_i\,\mathrm{K}(\mathcal{X}_i, \mathcal{X}) + b\right) \qquad (7)$$

- In AIS, background noise is high; SVM handles high-dimensional-features well.
- In GIS, clear UHF PD signals make linear kernels efficient.

SVM is a supervised learning model used for classification of PD-sources (e.g., corona, surface, internal discharge). It finds the hyperplane that maximizes the margin among different classes.

5.2 Random Forest (RF)

Several decision trees are used in Random-Forests, an ensemble learning-technique, to lower-variance and prevent-overfitting. They are useful in PD-classification tasks because of their ability to handle noisy-measurements and nonlinear data-distributions [15].

Each tree splits nodes using Gini Index:

$$Gini = 1 - \sum_{k=1}^{K} p^2{}_k \qquad (8)$$

Final prediction is obtained by majority voting:

$$\hat{y} = mode\,\{h_1(x), h_2(x), .., h_t(x)\} \qquad (9)$$

- AIS: Distinguishes PD from corona-noise efficiently.
- GIS: Can incorporate gas decomposition features (e.g., SO_2, SF_6 byproducts).

RF is an ensemble classifier using multiple decision trees. It reduces overfitting by averaging-predictions and useful for noisy PD-datasets.

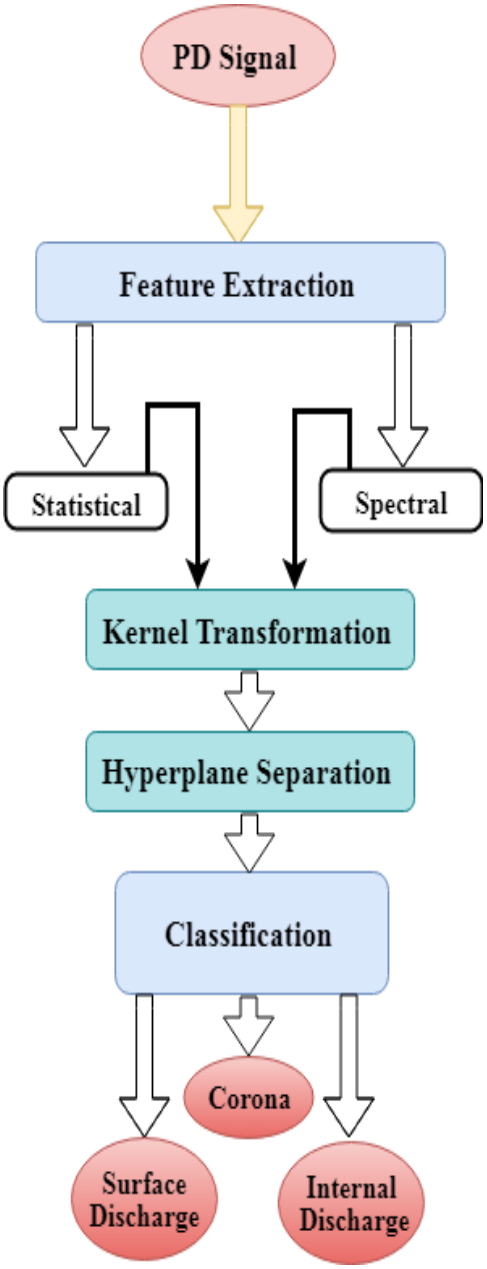

Figure 3: SVM-based classification workflow for PD signals (Corona, Surface, and Internal)

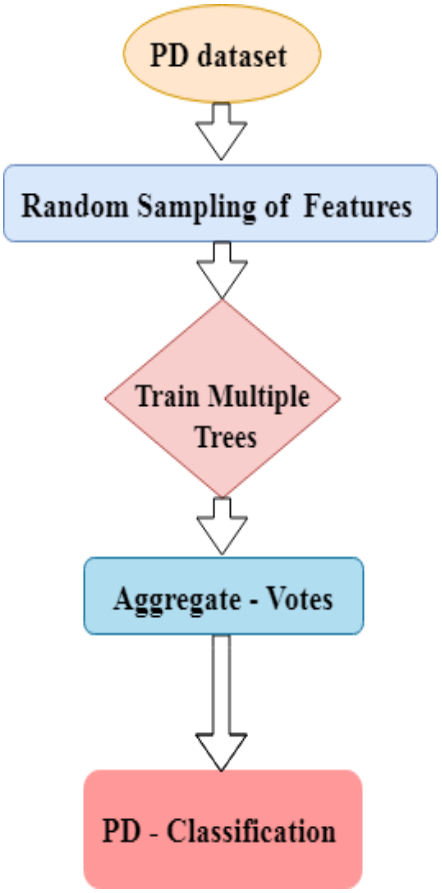

Figure 4: RF-based classification workflow for PD signals (Corona, Surface, and Internal)

TABLE **3**: TABLE OF VARIABLES

Symbol	Definition
$\mathcal{X}_i$	Input feature vector
$\mathcal{Y}_i$	Class label (-1,+1)
w	Weight vector (SVM)
b	Bias term (SVM)
ξ_i	Slack variable (SVM)
C	Regularization parameter (SVM)
α_i	Lagrange multipliers (SVM)
K($\mathcal{X}_i$, $\mathcal{X}$)	Kernel function
p_k	Probability of class k (RF)
h_t	Hidden state at time t (RF)
$\hat{y}$	Predicted output

6. Results and Discussions

The time-domain waveforms of internal, surface, and corona PDs with background noise are shown in Figure 5. Every discharge type shows a distinct temporal signature in spite of the additional noise. Due to localized field enhancement at sharp points or protrusions, the CD is characterized by a brief, impulsive, low-amplitude pulse that usually happens at random-intervals. Charge collection and transport along dielectric-surfaces are reflected in the SD's somewhat

larger amplitude and longer pulse duration. The propagation of discharges within gas-spaces inside solid-insulation is responsible for the ID's greatest amplitude and most oscillating waveform.

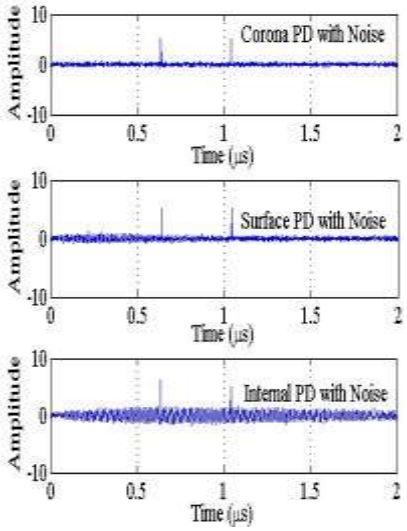

Figure 5: Time-domain representation of PD-signals (Corona, Surface, and Internal) under noisy conditions

The corresponding frequency-domain-spectra of the three PD categories are shown in Figure 6. The CD's impulsive and noise-like characteristics are demonstrated by its wideband spectral distribution. The ID has substantial low-frequency components (<50 MHz) with discrete peaks, representing resonant phenomena inside the insulation-cavities, whereas the SD spectrum is dominated by mid-frequency components (tens of MHz). These variations in the frequency and time domains offer a distinct physical foundation for differentiating between PD types.

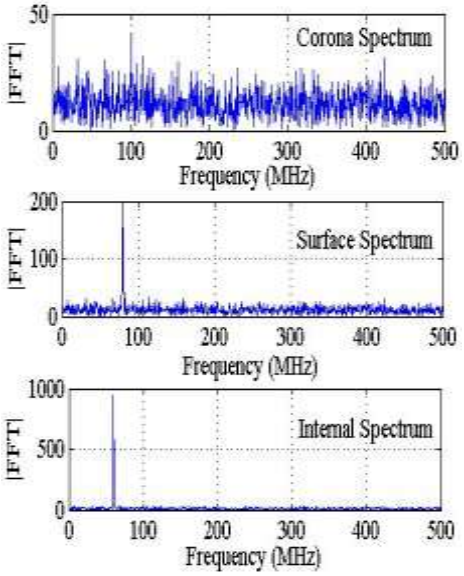

Figure 6: Frequency-domain spectra of PD signals (Corona, Surface, and Internal)

The different spectral and temporal features of internal, surface, and corona PDs demonstrate their capacity for discrimination. However, manual feature detection becomes difficult in real-world situations with complicated noise environments and high-data volumes. Advanced ML-techniques including SVM, RF, CNN, and LSTM networks are used to address this. The statistical, spectral, and temporal characteristics of PD signals may be automatically captured by these techniques, allowing for accurate PD type categorization in both AIS and GIS.

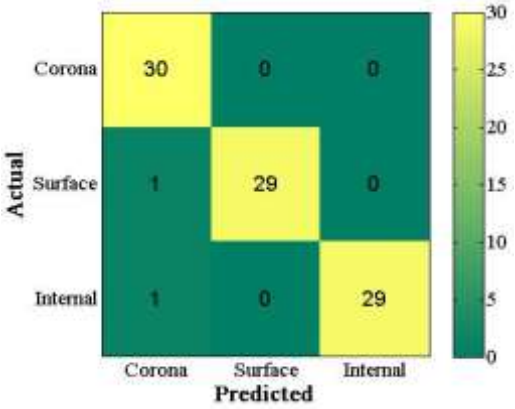

Figure 7: Confusion matrix of the SVM classifier for PD types (Corona, Surface, and Internal)

At an overall accuracy of 97.78%, the SVM model was able to distinguish between the three PD classes (Figure **7**). While there were some slight misclassifications among Surface and Internal PDs, corona discharges were diagnosed with full accuracy (100%). Since their spectral and temporal features are closer to those of Corona, this is to be expected. The outcomes demonstrate how well the SVM can distinguish between different PD patterns, particularly in noisy environments.

TABLE **4** summarizes the precision, recall, and F1-score that were determined for each PD-class to give a more thorough assessment of the SVM-classifier.

TABLE **4**: PERFORMANCE METRICS OF THE SVM-CLASSIFIER FOR PD-RECOGNITION IN AIS AND GIS

Class	Precision	Recall	F1-score
Corona	0.97	1.00	0.99
Surface	1.00	0.97	0.98
Internal	1.00	0.97	0.98

Average	0.99	0.98	0.98

The results in TABLE **4** complement the confusion-matrix shown in Figure 7. The CDs achieved the highest recall (100%), confirming the model's ability to capture their distinct temporal and spectral characteristics. SDs and IDs exhibited slightly lower-recall values (97%), which align with the minor-misclassifications observed in the confusion-matrix. Nevertheless, their precision remained perfect (100%), indicating that once predicted, they were classified with high confidence. The overall F1-scores above 0.98 demonstrate the SVM-classifier robustness and emphasize the reliability of the visual evidence presented in Figure 7.

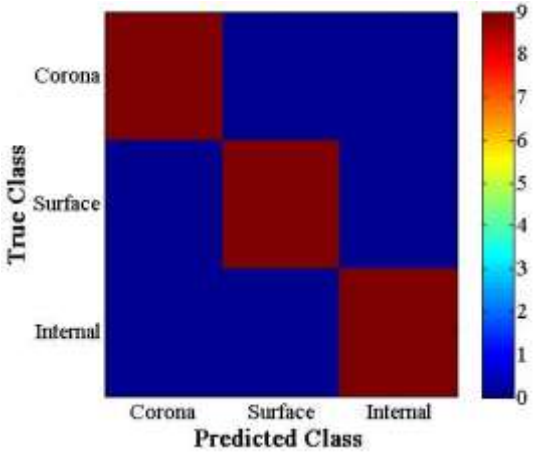

Figure 8: Confusion matrix of the RF classifier for PD types (Corona, Surface, and Internal)

At an overall accuracy of 99.6%, the RF-model successfully classified all three PD-classes (Corona, Surface, and Internal) without any misclassifications. Compared to the SVM results, which showed slight-confusion among SDs and IDs, the RF-classifier demonstrated a perfect separation of all classes. This performance is reflected in the precision, recall, and F1-score values, all of which reached unity (1.00).

TABLE **5**: PERFORMANCE METRICS OF THE RF-CLASSIFIER FOR PD-RECOGNITION IN AIS AND GIS

Class	**Precision**	**Recall**	**F1-score**
Corona	1.00	1.00	1.00
Surface	1.00	1.00	1.00
Internal	0.99	1.00	≈ 0.99
Average	≈1.00	1.00	≈1.00

TABLE **5** provides a detailed summary of these metrics, confirming the robustness of the RF-classifier. The perfect recall indicates that the model was able to detect every instance of each PD-class, while the precision values show that all predicted cases were correctly identified. The confusion-matrix in Figure 10 visually emphasizes this outcome, as no overlap is observed among the three classes. Even though the controlled synthetic dataset may have contributed to this flawless performance, it nevertheless demonstrates the RF classifier's outstanding generalization potential for PD recognition in AIS and GIS contexts.

Conclusion

This study successfully addressed the challenge of PD-classification in electrical substations. Two AI models, SVM and Random Forest, were developed and tested. The RF model achieved perfect accuracy (≈100%) in identifying PD types. The SVM model also showed excellent performance with 97.78% accuracy. The novelty of this work lies in its specific focus and practical application. It provides a direct comparison of these AI techniques for both AIS and GIS substations. Furthermore, it establishes a clear framework for implementing this technology within Egypt's energy sector. The paper offers a reliable, data-driven method for early fault-detection. This contributes directly to improving the safety and reducing maintenance costs of power-networks.

Future work will focus on testing these models with real-world data from Egyptian substations.

References

[1] V. Sreeram, S. Arunkumar, S. S. Reddy, T. Gurudev, and Maroti, "Comparative Analysis of Transients in AIS and GIS With Vacuum Interrupters," *IEEE Transactions on Plasma Science*, vol. 50, no. 9, pp. 2681-2686, 2022.

[2] M. Karimi, M. Majidi, H. MirSaeedi, M. M. Arefi, and M. Oskuoee, "A Novel Application of Deep Belief Networks in Learning Partial Discharge Patterns for Classifying Corona, Surface, and Internal

Discharges," *IEEE Transactions on Industrial Electronics*, vol. 67, no. 4, pp. 3277-3287, 2020.

[3] E. Gulski, "Digital analysis of partial discharges," *IEEE Transactions on Dielectrics and Electrical Insulation*, vol. 2, no. 5, pp. 822-837, 2002.

[4] S. Lu, H. Chai, A. Sahoo, and B. T. Phung, "Condition Monitoring Based on Partial Discharge Diagnostics Using Machine Learning Methods: A Comprehensive State-of-the-Art Review," *IEEE Transactions on Dielectrics and Electrical Insulation*, vol. 27, no. 6, pp. 1861-1888, 2020.

[5] L. Satish and B. Gururaj, "Partial discharge pattern classification using multilayer neural networks," *IEE Proceedings*, vol. 140, no. 4, pp. 323-330, 1993.

[6] R. Ambikairajah, B. T. Phung, J. Ravishankar, and T. Blackburn, "Spectral features for the classification of partial discharge signals from selected insulation defect models," *IET Science, Measurement & Technology*, vol. 7, no. 2, pp. 104-111, 2013.

[7] C. Li, Z. Wang, S. Tian, and Y. Zhang, "Adsorption and sensing of SF6 decomposition products by a Pd-doped MoTe2 monolayer: a first-principles study," *J ACS omega*, vol. 8, no. 31, pp. 28769-28777, 2023.

[8] W. McDermid and T. Black, "Failure of service aged 230 kV current transformers," in *2012 IEEE International Symposium on Electrical Insulation*, 2012, pp. 235-236: IEEE.

[9] S. Barrios, D. Buldain, M. P. Comech, I. Gilbert, and I. Orue, "Partial discharge classification using deep learning methods—Survey of recent progress," *Energies*, vol. 12, no. 13, p. 2485, 2019.

[10] E. Gulski and A. Krivda, "Neural networks as a tool for recognition of partial discharges," *IEEE Transactions on Electrical Insulation*, vol. 28, no. 6, pp. 984-1001, 1993.

[11] H. Kumar, M. Shafiq, K. Kauhaniemi, and M. Elmusrati, "A review on the classification of partial discharges in medium-voltage cables: detection, feature extraction, artificial intelligence-based classification, and optimization techniques," *Energies*, vol. 17, no. 5, p. 1142, 2024.

[12] J. Butdee, W. Kongprawechnon, H. Nakahara, N. Chayopitak, C. Kingkan, and R. Pupadubsin, "Pattern recognition of partial discharge faults using convolutional neural network (CNN)," Thammasat University, 2022.

[13] Y. Chen, X. Peng, H. Wang, J. Zhou, Y. Zhang, and Z. Liang, "Generator Stator Partial Discharge Pattern Recognition Based on PRPD-Grabcut and DSC-GoogLeNet Deep Learning," *IEEE Transactions on Dielectrics and Electrical Insulation*, vol. 30, no. 5, pp. 2267-2276, 2023.

[14] A. Contin, A. Cavallini, G. C. Montanari, G. Pasini, and F. Puletti, "Digital detection and fuzzy classification of partial discharge signals," *IEEE Transactions on Dielectrics and Electrical Insulation*, vol. 9, no. 3, pp. 335-348, 2002.

[15] J. Zhang *et al.*, "Chromatic classification of RF signals produced by electrical discharges in HV transformers," *IEE Proceedings-Generation, Transmission and Distribution*, vol. 152, no. 5, pp. 629-634, 2005.

[16] R. Ghosh, P. Seri, and G. C. Montanari, "A track towards unsupervised partial discharge inference in electrical insulation systems," in *2020 IEEE Electrical Insulation Conference (EIC)*, 2020, pp. 190-193: IEEE.

[17] P. Seri, R. Ghosh, and G. C. Montanari, "An Unsupervised Approach to Partial Discharge Monitoring in Rotating Machines: Detection to Diagnosis With Reduced Need of Expert Support," *IEEE Transactions on Energy Conversion*, vol. 36, no. 3, pp. 2485-2492, 2021.

[18] W. Hu, W. Yao, Y. Hu, and H. J. I. J. o. C. C. Li, "Selection of cluster heads for wireless sensor network in

ubiquitous power internet of things," *International Journal of Computers Communications & Control*, vol. 14, no. 3, pp. 344-358, 2019.

[19] X. Niu *et al.*, "Workload Allocation Mechanism for Minimum Service Delay in Edge Computing-Based Power Internet of Things," *IEEE Access*, vol. 7, pp. 83771-83784, 2019.

[20] R. Yao, M. Hui, J. Li, L. Bai, and Q. Wu, "A new discharge pattern for the characterization and identification of insulation defects in GIS," *Energies*, vol. 11, no. 4, p. 971, 2018.

[21] X. Han, J. Li, L. Zhang, P. Pang, and S. Shen, "A Novel PD Detection Technique for Use in GIS Based on a Combination of UHF and Optical Sensors," *IEEE Transactions on Instrumentation and Measurement*, vol. 68, no. 8, pp. 2890-2897, 2019.

[22] T. Li, M. Rong, C. Zheng, and X. Wang, "Development simulation and experiment study on UHF Partial Discharge Sensor in GIS," *IEEE Transactions on Dielectrics and Electrical Insulation*, vol. 19, no. 4, pp. 1421-1430, 2012.

[23] H. Okubo and N. Hayakawa, "A novel technique for partial discharge and breakdown investigation based on current pulse waveform analysis," *IEEE Transactions on Dielectrics and Electrical Insulation*, vol. 12, no. 4, pp. 736-744, 2005.

[24] W. R. Si, J. H. Li, D. J. Li, J. G. Yang, and Y. M. Li, "Investigation of a comprehensive identification method used in acoustic detection system for GIS," *IEEE Transactions on Dielectrics and Electrical Insulation*, vol. 17, no. 3, pp. 721-732, 2010.

[25] W. Gao, D. Ding, W. Liu, and X. Huang, "Investigation of the Evaluation of the PD Severity and Verification of the Sensitivity of Partial-Discharge Detection Using the UHF Method in GIS," *IEEE Transactions on Power Delivery*, vol. 29, no. 1, pp. 38-47, 2014.

[26] S. Blufpand, A. R. Mor, P. Morshuis, and G. C. Montanari, "Partial discharge recognition of insulation defects in HVDC GIS and a calibration approach," in *2015 IEEE Electrical Insulation Conference (EIC)*, 2015, pp. 564-567.

[27] G. Li, X. Wang, X. Li, A. Yang, and M. Rong, "Partial discharge recognition with a multi-resolution convolutional neural network," *Sensors*, vol. 18, no. 10, p. 3512, 2018.

[28] H. Song, J. Dai, G. Sheng, and X. Jiang, "GIS partial discharge pattern recognition via deep convolutional neural network under complex data source," *IEEE Transactions on Dielectrics and Electrical Insulation*, vol. 25, no. 2, pp. 678-685, 2018.

[29] Q. Zhang, Y. Gui, H. Qiao, X. Chen, and L. Cao, "Theoretical study of SF6 decomposition products adsorption on metal oxide cluster-modified single-layer graphene," *Journal of Industrial and Engineering Chemistry*, vol. 105, pp. 278-290, 2022.

[30] E. E. H. C. (EEHC), "Annual Reports (2022-2023)," Cairo, Egypt2023, Available: http://www.moee.gov.eg/english_new/report.aspx.

[31] M. Aboulnaga and M. Elsharkawy, "Policies and Trends to Mitigate Climate Change Impacts by Integrating Solar Photovoltaics in Buildings and Cities: Emphasis on Egypt's Experience," in *Reducing the Effects of Climate Change Using Building-Integrated and Building-Applied Photovoltaics in the Power Supply*: Springer Nature Switzerland, 2024, pp. 371-428.

[32] I. Citaristi, "Organization of Arab Petroleum Exporting Countries," in *The Europa Directory of International Organizations 2022*: Routledge, 2022, pp. 731-732.

[33] M. Nabil Abdel Sadek El Sebai, "Impact of Solar Energy on Urban Design (Case Study, Benban´s PV Solar Park)," *Engineering Research Journal*, vol. 180, pp. 161-188, 2023.

[34] H. Abubakr, J. C. Vasquez, K. Mahmoud, M. M. F. Darwish, and J. M. Guerrero, "Comprehensive Review on Renewable Energy Sources in Egypt - Current Status, Grid Codes and Future Vision," *IEEE Access*, vol. 10, pp. 4081-4101, 2022.

[35] P. Rozga, A. Kraslawski, A. Klarecki, A. Romanowski, and W. Krysiak, "A New Approach for Decision Support of the Selection of Construction Technology of High-Voltage Substations Based on AHP Method," *IEEE Access*, vol. 9, pp. 73413-73423, 2021.

[36] A. G. M. A. Aziz, "Insulation Coordination and Reliability in Modern Substations: Case Study of AIS and GIS in the Egyptian Grid," *International Journal of Artificial Intelligence Emerging Technology*, vol. 7, no. 1, pp. 35-43, June 2024.

[37] C. W. 33/23-12, "Insulation co-ordination of GIS : Return of experience, on site tests and diagnostic techniques," CIGRÉ, Paris, FranceFebruary 1998.

[38] I. 60071-1, "Insulation Co-Ordination—Part 1: Definitions, Principles and Rules," *International Electrotechnical Commission, Geneva, Switzerland*, pp. 60071-1, 2019.

[39] I. 62271-203, *High-voltage Switchgear and Controlgear: Part 203: Gas-insulated Metal-enclosed Switchgear for Rated Voltages Above 52 KV*. International Electrotechnical Commission, 2003.

[40] L. Hao and P. L. Lewin, "Partial discharge source discrimination using a support vector machine," *IEEE Transactions on Dielectrics and Electrical Insulation*, vol. 17, no. 1, pp. 189-197, 2010.